

# Lecture 7: From the Photosphere to the Hot Corona

## Aims, learning outcomes, and overview

**Aim:** To review the layers and phenomena of the solar atmosphere and then to describe the coronal heating problem, including the observational requirements, proposed models, and associated successes and shortcomings.

**Learning outcomes:** At the end of this lecture, students are expected to:

- describe qualitatively the properties, main phenomena, and qualitative interpretations of the chromosphere, transition region, and corona;
- appreciate and explain qualitatively the connection between the magnetic field and coronal heating;
- understand the “velocity filtration” exospheric model for coronal heating;
- be able to explain qualitatively the role of acoustic waves and shocks in spicules and chromospheric heating;
- have a qualitative understanding of wave heating models;
- have a qualitative understanding of DC heating and magnetic reconnection processes.

### Overview:

This lecture addresses the atmosphere of the Sun, its various layers and properties, and then the heating of these layers. A large number of possible mechanisms have been proposed, but there is no consensus of opinion, and the problem of heating the Sun’s corona remains an outstanding question in space physics and astrophysics. Heating of the chromosphere is also not well understood, although heating by shocks associated with spicules appears increasingly attractive. After describing the observational constraints faced by heating models, these models are briefly summarized and explained, together with their attractive aspects and shortcomings.

## 7.1 The Sun’s Atmosphere

The Sun’s atmosphere is usually separated into three layers above the photosphere, the so-called chromosphere, transition region, and then the corona. Some of the coronal material flows out into the solar wind, discussed in future lectures. Each region has different phenomena and has a different range of characteristic temperatures, densities, and other plasma characteristics and is often observed at distinct

wavelengths. Each region is believed to occur in a characteristic range of altitude above the photosphere.

The photosphere is primarily neutral and collisional, with a relatively small ionization fraction. With increasing altitude the medium becomes less collisional and more highly ionized, due to decreasing density and increasing temperatures (on average). Eventually the corona itself is at least a million degrees Kelvin and is collisionless.

The chromosphere and transition region are both extremely time-variable and small in altitude range. It is legitimate to ask whether the time-variability is intrinsic to the physics and whether the time-averaged pictures of the chromosphere and transition region are useful. Put another way, what are the “filling” fraction and energy inputs of the time-varying regions compared to the “whole” and are there any parts of the region that actually have the properties of the average region?

### 7.1.1 Chromosphere and spicules

The chromosphere is the layer of the atmosphere just above the photosphere. It gains its name from its colourful appearance just before and after a total eclipse, during which time spectral lines that are normally seen in absorption are seen in emission. The chromosphere can be observed on the disk in the  $H\alpha$  (Balmer) line, which reveals a wealth of filamentary structure that aligns locally with the magnetic field (Figure 7.1).



Figure 7.1: This eclipse image shows the chromosphere as the ruby ring around the dark silhouette of the Moon. The corona is the white cloud further out. Note the many approximately radial features.

The chromosphere has a temperature of about  $10^4$  K, based on the characteristic spectral lines emitted, and a thickness of a few thousand kilometres. Since the photosphere is much cooler, and has a temperature that increases with depth, and the upper chromosphere is much hotter, there must be a *temperature minimum region* in the chromosphere. Figure 7.2 shows the temperature and number density profiles of the low solar atmosphere. Note the very abrupt nature of the transition region. The temperature of the minimum region is about 4000 K and it occurs about 500 km above the photosphere. The reason for the enhanced temperature of the chromosphere is unclear.

It has been known since the 1940s that the solar corona, which lies above the chromosphere, is much hotter again, at several million Kelvin. The corona is heated by an (unknown) mechanism that continually pumps energy from the cooler regions

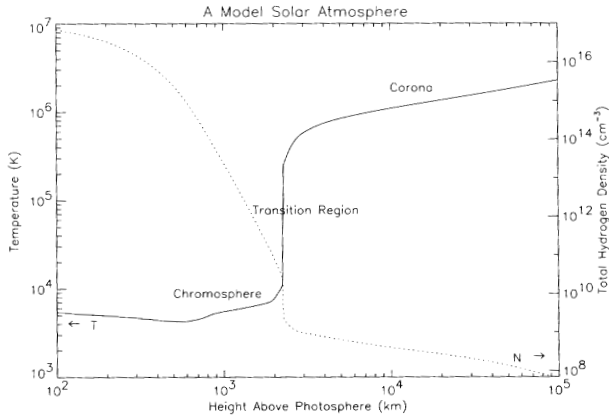


Figure 7.2: The temperature profile of the low solar atmosphere [Golub and Pasachoff, 1997].]

below to the hotter ones above, as discussed in detail below. The chromosphere is heated to some extent by conductive flow back down the temperature gradient from the overlying corona, but additional local heating is also required.

At the limb, numerous fine jets of material called *spicules* are observed to move through the chromosphere and into the transition region and lower corona. The path and shape of each spicule is believed to show magnetic field lines. Spicules are a very plausible heating mechanism and source of plasma for the chromosphere and higher regions. Spicules last about 5 minutes, have a relatively small diameter of about 500 km or less, and move at about  $20 \text{ km s}^{-1}$ . They have temperatures of order 5000 - 20,000 K. It is estimated that over  $10^5$  spicules are active at any time on the Sun. It is relevant that spicules are found across the Sun, meaning below coronal holes, near sunspots and active regions etc.

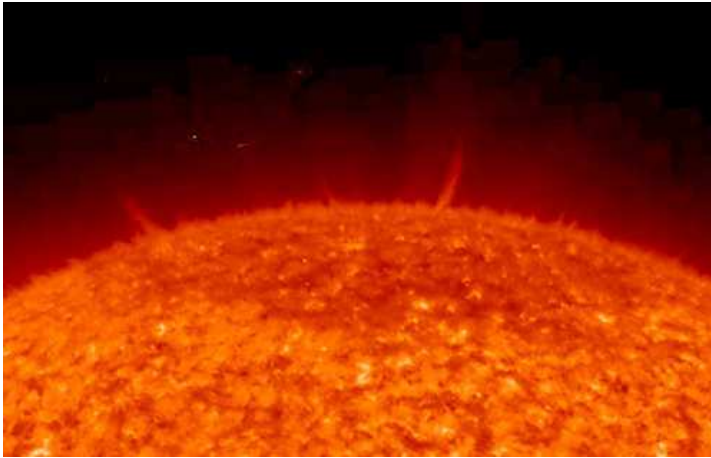


Figure 7.3: Observations from one of the STEREO spacecraft, showing multiple spicules moving from the low chromosphere into the corona.

Spicules show evidence for waves propagating along the magnetic field lines, associated with wave-like motions of the spicule body, and for shocks. Figure 7.4 shows recent simulations of sound waves moving up from the photosphere, perhaps excited by granular motions, that steepen into shock waves that heat plasma and

cause it to move upward, before sometimes falling back down. The top and bottom panels show the plasma temperature and velocity, respectively, from just below the photosphere into the corona. The top panel shows the million-degree corona (white region at top) suffused with reddish jets (temperatures of 20,000 K) that have very similar properties to spicules. In the bottom panel upflowing plasma is blue and downflowing plasma is red.

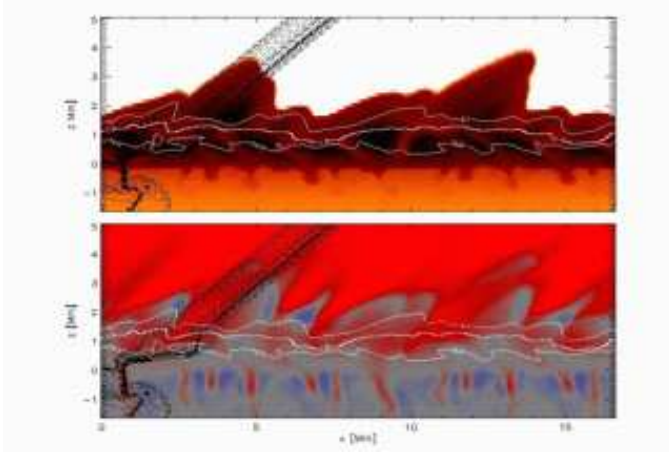


Figure 7.4: Fluid simulation of the region from below the photosphere to the corona, showing spicules produced by shocks derived from steepened sound waves excited by granulation motions.

*Exercise: use normal pressure balance across a shock moving at  $20 \text{ km s}^{-1}$  to estimate the downstream temperature (cf. Lecture 5) and compare the result with the chromospheric temperature.*

### 7.1.2 Transition region

The boundary between the relatively cool chromosphere and the million-degree corona is called the *transition region*. Simple atmospheric models predict that there is a very sharp transition, with density and temperature changing almost discontinuously (although their product, i.e. pressure, is almost constant). Observations in EUV provide indirect support for a thin transition region, although the actual height of the chromosphere is highly variable.

### 7.1.3 Corona

The solar corona is a diffuse (at the base of the corona the electron number density is about  $10^{15} \text{ m}^{-3}$ ), hot ( $T \approx 2 \times 10^6 \text{ K}$ ) plasma extending more than a solar radius above the surface of the Sun. The corona merges with the *solar wind*. The corona is only visible in white light during total eclipses, because its intensity is about  $10^{-6}$  of that of the Sun's disk (roughly the brightness of the full moon). Figure 7.5 illustrates this situation.

Total eclipses are rare (they occur about twice every three years), so they are of limited use in studying the corona. A *coronameter* is a device which permits the routine observation of white light from the corona by occluding the disk of the Sun and exploiting the linear polarisation introduced by Thomson scattering of the photons off coronal electrons. Coronameters are used to study the structure of the corona and of the inner solar wind, and also are used to observe *corona mass*

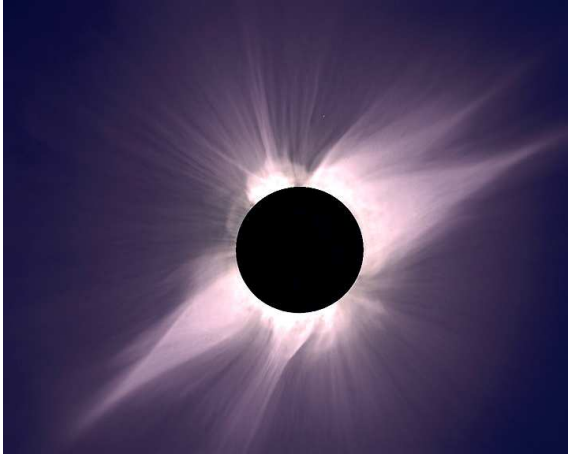


Figure 7.5: An eclipse image of the Sun, showing extended magnetic structures in the solar corona [from <http://cfa-www.harvard.edu>].

*ejections*, or *CMEs*, dynamic events in which mass and magnetic field is expelled from the Sun. These events play an important role in *space weather*.

The corona is best observed in the extreme ultraviolet and X-ray regions of the spectrum, but because the atmosphere blocks these short wavelengths, the observations must be made from space. An X-ray image of the Sun is shown in Figure 7.6. Soft X-ray and UV emission from the corona consists of thermal bremsstrahlung (‘free-free emission’), which produces a continuum, as well as line emission. Skylab provided the first detailed study of the solar corona in soft (low-energy) X-rays, and revealed that the soft X-ray emitting plasma of the corona is everywhere structured into loops, except in dark *coronal holes* that occur predominantly at the poles (coronal holes are visible in Figures 7.6 and 7.7. Soft X-ray loops are believed to delineate the magnetic field, and represent *closed field* regions, i.e. magnetic flux tubes in which the field is anchored at the photosphere at both ends. The brightest loops occur around active regions, pointing to the central role of the magnetic field in coronal heating. Coronal holes are *open field* regions, where the magnetic field at the photosphere has a particular polarity, and leaves the Sun, passing into interplanetary space. The corona in X-ray also reveals other structures. Extended magnetic configurations with cusp-like shapes (*helmet streamers*) are seen in Figure 7.6. *Prominences* are long-lived intrusions of dense, cool gas that arise due to a radiative instability, and are suspended in the hot corona by magnetic forces. When they appear on the disk they are called *filaments*.

The magnetic field determines the structure of much of the solar corona because the ratio of gas pressure to magnetic pressure (the plasma beta, introduced in Lecture 2), is very small. Hence in most locations in the solar corona, magnetic forces dominate over pressure and gravitational forces. In such static situations, e.g. in observed soft X-ray loops, the MHD equation of motion [equation (2.37)] then collapses to the statement that the Lorentz force is zero,

$$(\nabla \times \mathbf{B}) \times \mathbf{B} = 0. \quad (7.1)$$

A magnetic field satisfying equation (7.1) is called a *force-free field*. Force-free fields have a current density  $\mathbf{J} = \mu_0^{-1} \nabla \times \mathbf{B}$  parallel to the magnetic field, so they satisfy

$$\nabla \times \mathbf{B} = \alpha \mathbf{B}, \quad (7.2)$$

where  $\alpha = \alpha(\mathbf{x})$  is a scalar function of position. Taking the divergence of equa-

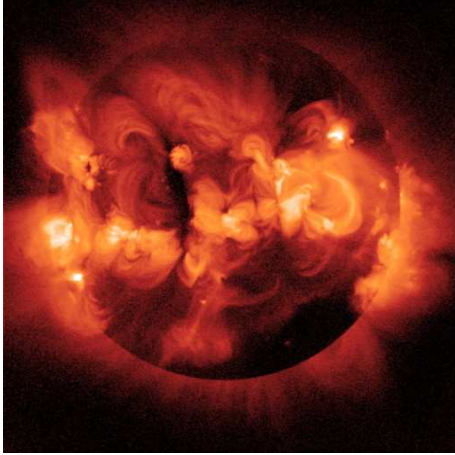


Figure 7.6: The Sun in X-rays, as observed by the Yohkoh satellite. The bright regions are closed field structures (loops) around solar active regions. The darker regions are coronal holes, where the magnetic field is open, i.e. leads out into the solar wind. [From <http://solar.physics.montana.edu/>.]

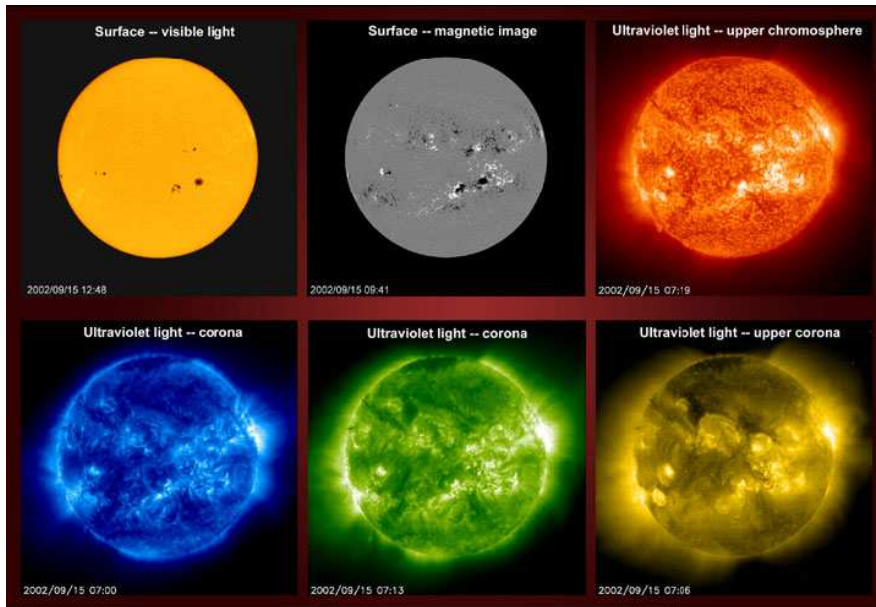


Figure 7.7: The Sun in many spectral bands, showing the importance of magnetic fields, sun spots, and active regions. [From the SOHO website.]

tion (7.2) gives

$$\mathbf{B} \cdot \nabla \alpha = 0, \quad (7.3)$$

which implies that  $\alpha$  is constant along a field line. The values of  $\alpha$  determine the currents which flow in the force-free field, since  $\alpha = \mu_0 J/B$ , where  $J$  is the magnitude of the current density. Equation (7.1) [or Equations (7.2) and (7.3)] is a non-linear equation in general, and is remarkably difficult to solve. Mathematically there are three classes of force-free fields, depending on the form of  $\alpha$ . *Linear* force-free fields are obtained when  $\alpha$  is a constant everywhere. The current-free, or *potential* case ( $\alpha = 0$ ) is a special example of linear force-free fields. Finally, when  $\alpha$  is different for different field lines, we have *non-linear* force-free fields. The linear and potential models are often used to represent fields in the solar corona. However, vector magnetic field measurements at the photosphere indicate that observed vertical currents are highly localized so that  $\alpha$  varies with position, pointing to the need for nonlinear force-free models.

The (open-field) corona is not gravitationally bound to the Sun, and is continually expanding, producing the *solar wind*. Lecture 8 describes the formation of the solar wind.

## 7.2 The heating problem

Observations of the solar corona during total eclipses allow the density scale height of the corona to be determined (cf. Figure 7.8), from which a high temperature for the corona can be inferred. These values were not widely believed because the photospheric temperature is so much smaller, the Sun is the ultimate source of the energy, and standard thermodynamic arguments. Only in the last century was the high temperature of the corona confirmed spectroscopically by Eddington in 1939 (following a suggestion of Grotrian), by interpreting puzzling coronal lines as emission from highly ionized states of iron, calcium and nickel.

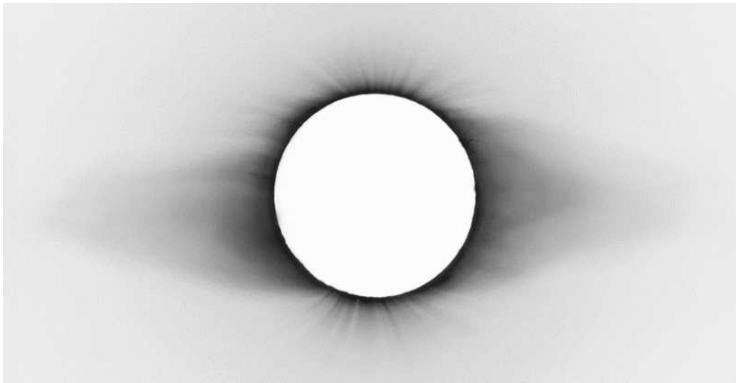


Figure 7.8: Photograph of an eclipse (shown in inverse), illustrating the large density scale height of the corona. [From <http://umbra.nascom.nasa.gov/eclipse/images/>. Photo by Fred Espenak.]

The central problem then is that the corona is much hotter than the Sun's photosphere, but the energy to heat the corona originates below the photosphere. This temperature inversion above the Sun's surface rules out equilibrium thermal transport (or standard thermodynamic) processes since heat should be flowing from a hotter body to a cooler body. One or more non-thermal (or non-equilibrium) processes are therefore required to heat the corona, the chromosphere, and the transition region.

### 7.3 Observational Constraints on Coronal heating and Solar Activity

There are many detailed observational constraints on the heating of the solar atmosphere, especially the corona, and it is not possible to examine them all in detail here. For instance, if profiles for the plasma temperature, density, and composition are assumed then losses due to radiation and heat conduction can be calculated and compared with the energy radiated directly from the photosphere, the energy in the convective motion of granulation cells, the photospheric magnetic field, spicules etc. Detailed reviews can be found elsewhere [e.g., Golub and Pasachoff, 1997; Ulmschneider and Kalkofen, 2003; Cranmer 2009]. Attention is focused here on some important qualitative results for the Sun and other stars.

The magnetic field appears to be fundamental for coronal heating. Most heating occurs in active regions, where the field is very intense (see Figure 7.7), and small scale heating in the low atmosphere is associated with magnetic flux elements observed at the photosphere. Moreover, the brightness of the whole X-ray corona varies in step with the *solar cycle*, the periodic (11-year) variation in strength of the Sun's magnetic field, as shown in Figure 7.9. Further, Fisher et al. (1998) determined that X-ray emission is well correlated with the total (unsigned) magnetic flux of active regions.

These observations indicate a close relationship between magnetic fields and coronal heating, but historically opinion was divided as to whether the magnetic field plays an active or a passive role in the heating process. In the active picture, the energy for heating derives from the field itself, whilst in the passive picture, the field is essentially a conduit for the transport of energy from the subphotosphere. The consensus now appears to be that the role is active, based on the ubiquitous association of heating with field, on all scales. Independent of this, any viable model needs to account for heating in the two types of magnetic structures: open regions (coronal holes and streamers), and closed regions (loops). It is possible that different mechanisms operate in the different regions.

Studies of other stars may also provide clues to the heating process. Observations show that the X-ray luminosity of late-type stars is correlated with the rotation rate of the stars, as shown in Figure 7.10. X-ray flux is also correlated with the surface magnetic flux of solar-type stars. These observations once again link coronal heating to the magnetic dynamo, which relies upon convection and the internal rotation of a star to produce magnetic fields. (See Lecture 6.) Stellar observations have also motivated recent progress in understanding chromospheric heating, as discussed in § 7.3.1.

Figure 7.11 shows plots of observed emission in two chromospheric lines for a variety of stars. The points are separated into two groups — low and high activity stars. This suggests that there are at least two operating mechanisms, one of which works only for high activity stars. It is widely believed that active stars are those with higher rotation and/or magnetic fields, implying that the mechanism for active stars involves the magnetic field. Ulmschneider and Kalkofen [2003] argued that the low activity points agree reasonably well with a model based on heating by acoustic (sound) waves that steepen into shocks and thereby heat the plasma (cf. spicules). Ulmschneider and Kalkofen were also able to obtain reasonable agreement with the high activity points using a model with acoustic heating plus heating due to magnetic waves in thin flux tubes.

Thus, there is evidence for at least 2 mechanisms being active in stars, one of which is strongly dependent on magnetic fields and one that involves shocks resulting from steepening of sound waves.

We come back to the Sun now, with observations from the UVCS instrument



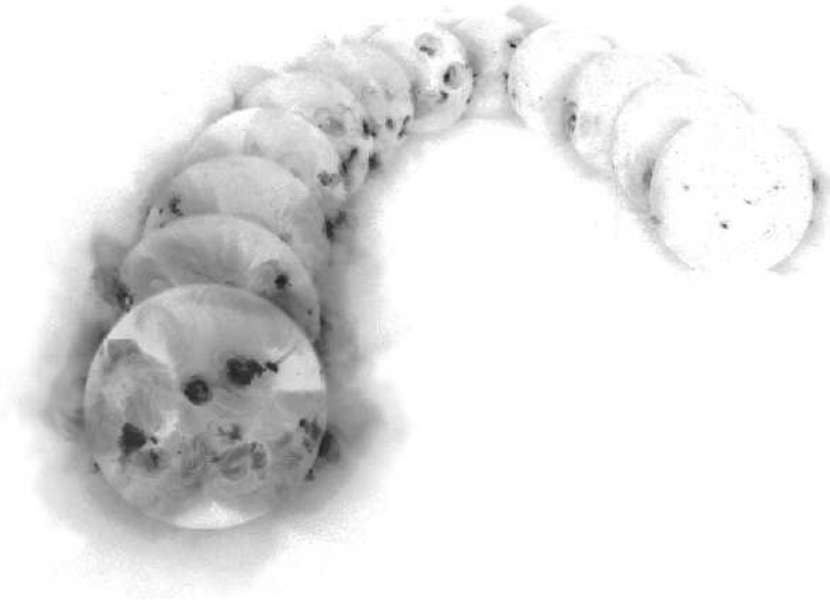


Figure 7.9: A mosaic of twelve X-ray images of the Sun between 1991 and 1995 at 120-day increments. The year 1991 was close to a solar maximum (when the magnetic field of the Sun is strongest), and 1995 was close solar minimum. The whole corona is observed to diminish with the cycle. [Picture by G.L. Slater and G.A. Linford, Lockheed Martin Space and Astrophysics Laboratory.]

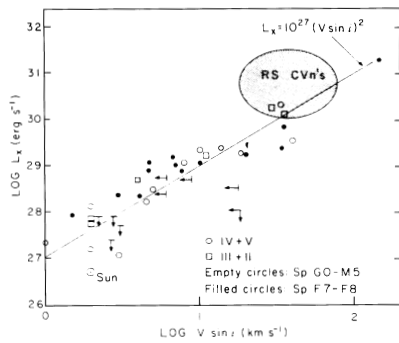


Figure 7.10: X-ray luminosity versus rotation rate for late-type stars [Golub and Pasachoff, 1997].

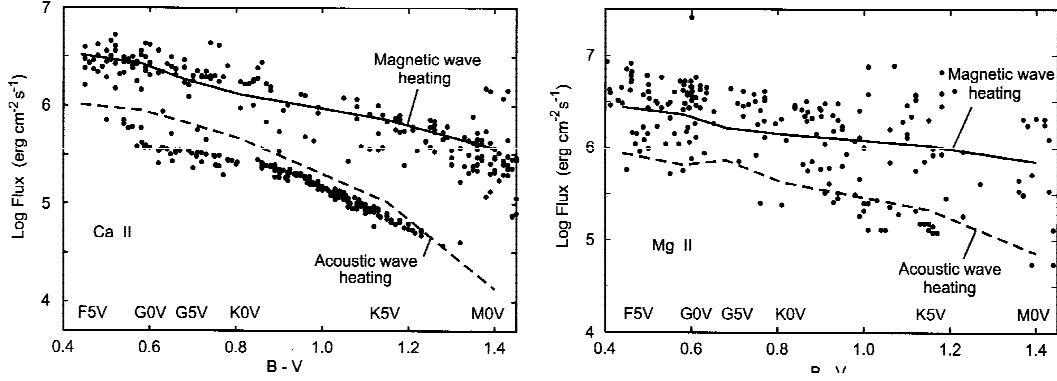


Figure 7.11: Fluxes in chromospheric lines for various stars. [Ulmschneider and Kalkofen, 2003].

on the SOHO spacecraft. Figure 7.12 illustrates at a glance the necessity for at least 1 kinetic heating process to be active in the corona [Cranmer, 2009]. Evidence for kinetic processes includes the following. First, protons are heated more strongly than electrons, by about a factor of 2, whereas a fluid process would lead to identical heating. Second, heavy ions (oxygen etc.) are heated much more strongly than the protons and the electrons, with the oxygen temperatures in excess of 200 MK - over a factor of 10 hotter than the Sun's core. Third, the ion heating appears to be significantly perpendicular to  $\mathbf{B}$ , with UVCS inferring temperature anisotropies up to  $T_{\perp}/T_{\parallel} \approx 10$ .

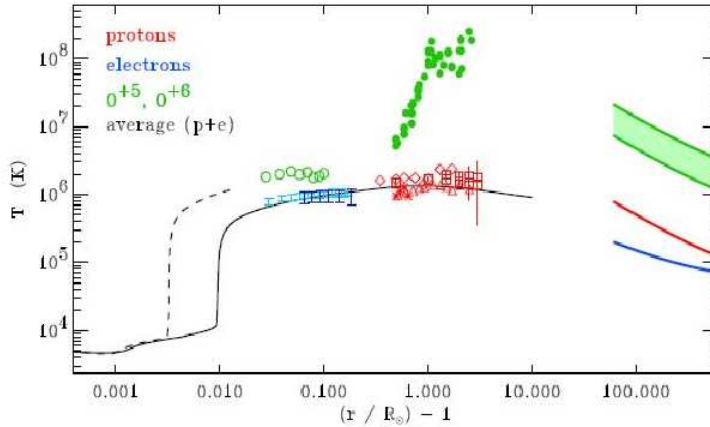


Figure 7.12: Radial dependence of observed and model temperatures in polar coronal holes and fast wind streams [Cranmer, 2009]. Dashed and solid curves show a semi-empirical model and turbulence-driven theoretical model, respectively. Electron temperatures are from off-limb SUMER data (blue symbols) and the proton (red symbols) and perpendicular  $O^{5+}$  (green symbols) temperatures from UVCS data. The in situ Helios measurements are shown with the curves beyond  $100R_S$ .

Figure 7.12 provides evidence for at least 2 heating processes also. One is required to produce the rapid increase in  $T_e$  and  $T_i$  below an altitude of  $0.1R_S$  to coronal temperatures. The second is required near an altitude of  $1R_S$ , where the heavy ions appear to be heated preferentially. Note that proton temperatures do

not appear to be available below this altitude, so it is unclear whether  $T_e > T_p$  or not below this altitude.

The relationship of the heating to the coronal plasma outflows that form the solar wind (next Lecture) is illustrated in Figure 7.13. It appears that the two are correlated. Moreover, the black curves show fluid models based on MHD with appropriate heating and momentum deposition terms added, as alluded to in Lecture 6. The good agreement of the proton and "blob" speeds with the models implies that we have a reasonable theoretical framework for understanding the heating and acceleration of the coronal plasma into the solar wind, even if most of the detailed mechanisms remain the subject of active research.

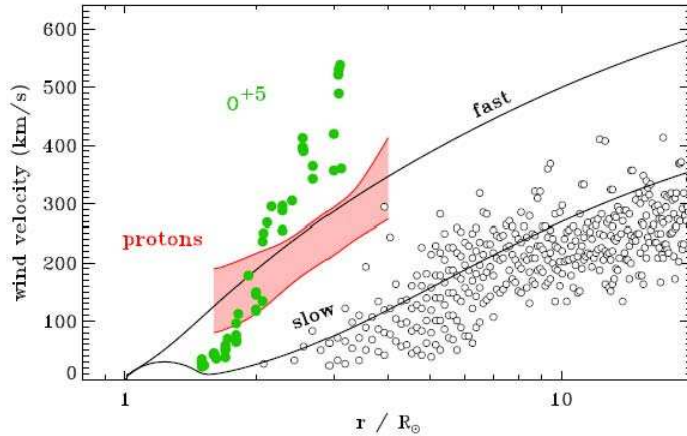


Figure 7.13: Radial dependence of plasma outflow speeds [Cranmer, 2009]. UVCS data for protons (red symbols) and  $O^{5+}$  ions (green) from UVCS data for polar coronal holes. Solid curves show the results of fluid models for fast and slow wind speeds, while open circles show speeds of "blobs" in LASCO coronagraph images above equatorial streamers.

## 7.4 Heating Mechanisms

Modern mechanisms for heating the chromosphere, transition region, and corona can be classified in several classes: the kinematic model of "velocity" filtration [Scudder, 1992,1994], heating by shocks, heating by waves, Joule heating by currents in loops and current sheets, and magnetic reconnection. As well as explaining heating, these mechanisms need to be at least compatible with outwards acceleration of some coronal plasma into the solar wind

At the present time there is no consensus on which mechanism or mechanisms are important for the Sun.

### 7.4.1 Velocity filtration

As mentioned above, the increase in temperature from the photosphere to the corona rules out equilibrium thermal energy transport processes. The simplest model for the corona is that it arises from the kinematic outward motion against gravity of particles with non-Maxwellian distribution functions in the chromosphere and transition region and that there is actually no heating mechanism in the standard sense [Scudder, 1992, 1994].

At one level the physics is very simple. Consider a distribution of individual electrons and ions in the chromosphere. Some of these may naturally have speeds greater than the gravitational escape speed  $V_{esc} = 2GM_S/R_S$  and so can move directly into the corona (ignoring collisions for the moment). For the same temperature there will be many more electrons than ions with speeds above  $V_{esc}$ , so these electrons can move out (ignoring electric field effects for the moment) into and beyond the corona. Now consider the distribution function as a function of height: the outmoving particles exchange kinetic energy for potential energy, thereby losing kinetic energy. Plotting an initially Maxwellian distribution as a function of directed kinetic energy  $E$  (negative values mean speeds directed in the negative direction), which then looks like two straight lines joined at  $E = 0$  with a gradient that depends on the temperature, then moving to different heights just corresponds to a particle moving from energy  $E_1$  to  $E_2$  with  $E_2 - E_1$  the change in kinetic energy corresponding to the change in height and potential energy. It is then easy to see by Liouville's theorem that an element of phase space in Figure 7.14 moves at constant height from  $E_1$  to  $E_2$ , unless  $E_2 \leq 0$  in which case the phase space element is removed (meaning that the particles had insufficient energy to reach the location). Accordingly the particle distribution function by removing elements of phase space with insufficient energy to reach there and moving the remaining phase space volumes to lower energy while retaining the local slopes etc. For a Maxwellian then, in Figure 7.14 (Left),  $f(E)$  remains a straight line with the same slope. Accordingly a Maxwellian distribution of electrons would retain the same temperature. However, if the initial distribution function were non-Maxwellian with more fast particles than a Maxwellian, then Figure 7.14 (Right) shows the same process would lead to the particles having a larger effective temperature. That is, the particles are heated as they move up the gravitation potential well. (For a non-Maxwellian distribution with fewer fast particles than a Maxwellian the result would be cooling with increased altitude.)

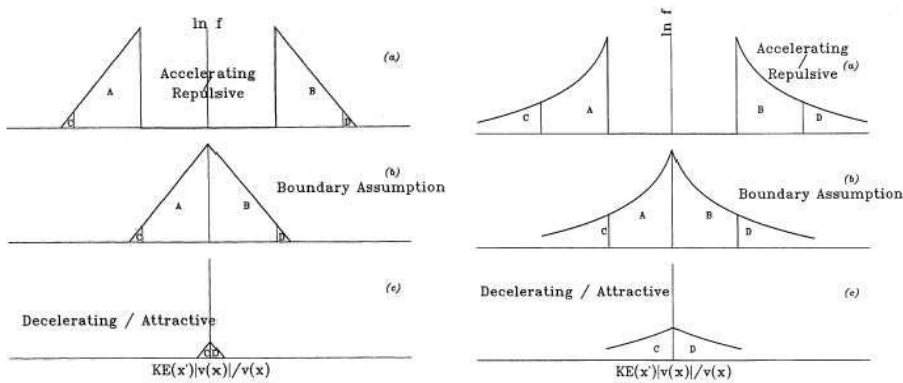


Figure 7.14: Distribution functions of particles as a function of (signed) kinetic energy from an initial condition (center panels) as they move in various potentials [Scudder, 1992]. (Left) A Maxwellian distribution of particles moving up a gravitational potential well (bottom two panels) does not change its temperature (the slope of the distribution function). (Right) A non-Maxwellian distribution with more fast particles than a Maxwellian increases in temperature as it moves up the gravitation well.

At one level the velocity filtration mechanism is so simple that it almost has to work. It does require a non-Maxwellian distribution function near the photosphere or in the chromosphere. While this can be argued against, since the photosphere

is collisional, the decrease in collisionality with increasing height and the decrease in the Coulomb collision rate with increasing particle speed (the mean free path is  $\propto v^3$  for large  $v$ ) makes it likely the distribution function becomes non-Maxwellian at large enough heights. Moreover, empirically in almost all regions of the solar wind and planetary magnetospheres the observed electron and proton distributions are non-Maxwellian with more fast particles than expected (the so-called Kappa distribution is usually observed, with  $f(v) \propto v^{-2(\kappa+1)}$ ). Another requirement is that Liouville's Theorem is satisfied, thereby placing limits on the amount of particle scattering and other losses that can be tolerated.

The foregoing arguments have considered electrons only and ignored ions. This is clearly not right, since the charge buildup due to electron loss would clearly set up an electric field that would retard the electrons and try to limit their loss. Crucially, this “ambipolar” electric field will also accelerate ions outward. In steady-state, then, the ambipolar electric field is indeed set up and it allows the ions to escape in equal numbers to the electrons so that the outflow is charge-neutral and does not build up charge on the Sun. This situation is described in more detail in the future lecture on Earth's ionosphere.

The Scudder model is novel, simple, and powerful, but has failed to catch on. It does not explain the basic association of heating with the magnetic field. Moreover, it predicts that the outflowing particles will have  $T_{\parallel} > T_{\perp}$ , due to conservation of magnetic moment for a magnetic field that decreases with altitude. This is inconsistent with the UVCS measurements described previously. However, velocity filtration could easily occur in conjunction with wave processes.

### 7.4.2 Shocks

The discussion above on spicules mentioned the idea that acoustic or other compressive waves can steepen nonlinearly as they propagate away from the Sun, turning into shocks that then heat and accelerate the plasma outwards. There is also evidence for this process in the chromosphere of other stars 7.11.

The basic argument for steepening goes as follows. The Sun and many other late-type stars have surface convection zones involving convection. There is a steep density gradient with radius, and acoustic waves propagating along this density gradient must increase in amplitude to conserve energy. The energy flux carried by an acoustic wave with amplitude  $v$  in a medium with density  $\eta$  and sound speed  $c_s$  is  $\mathcal{F}_s = \eta v^2 c_s$ . In the absence of damping the energy flux is conserved as the wave propagates upward. The sound speed varies only with temperature, and is almost constant near the base of the chromosphere. Assuming the density falls off exponentially,  $\eta \propto \exp(-z/H)$ , energy flux conservation implies  $v \propto \exp[z/(2H)]$ , and hence the velocity amplitude of the wave increases exponentially with height. As the velocity amplitude increases, nonlinear effects cause the wave to steepen into a sequence of shocks, which dissipate more rapidly than the original waveform.

### 7.4.3 Waves

Many proposals exist for specific wave modes to heat the chromosphere and corona. These include slow magnetoacoustic (or acoustic), Alfvén, fast magnetoacoustic waves, and ion cyclotron waves with wavenumbers and frequencies that differ by orders of magnitude. Their sources range widely as well, from waves excited by convective motions below and at the photosphere to waves produced by nonlinear processes to waves produced in magnetic reconnection regions or as a result of impulsive flows produced in reconnection regions. The ultimate source of the wave energy is believed to be mechanical energy at the photosphere. Recent reviews by Klimchuk [2006], Aschwanden [2008] and Cranmer [2009] are relevant.

Reflection of some wave energy by the sharp change in density in the transition region is important, both in limiting the energy input but also in terms of producing regions with both upgoing and downward waves that can interact nonlinearly to produce turbulence with smaller spatial scales (larger wavenumbers) and higher frequencies that are better able to resonantly interact with the plasma particles and heat them by Landau damping. Typically this heating is desired well above the transition region and it is relevant that Landau damping and refraction can prevent certain waves from reaching the corona if produced in the chromosphere or below, thereby necessitating generation by mode-conversion, nonlinear processes, or other mechanisms in the corona.

One might hope that the group velocities and refractive effects for these waves might provide natural explanations for the observed correlations between heating and magnetic fields, including loops. While Alfvén waves typically favour propagation along field lines, while fast mode waves can propagate obliquely and are refracted into denser regions (like loops and active regions), it appears that no firm conclusions can be drawn at this time.

Perhaps the most direct evidence for wave processes involves the strong perpendicular heating of high charge-state oxygen (and magnesium) ions in Figure 7.12 [Cranmer et al., 1999; Cranmer 2009]. This can be understood nicely in terms of resonant heating by the perpendicular electric fields of ion cyclotron waves (e.g., due to very high wavenumber Alfvén waves with high frequencies  $\approx 10 - 10^4$  Hz near  $\Omega_{ci}$  at  $r \approx 1.5R_S$ ). Heating at this height could provide additional acceleration of the solar wind (see Lecture 8).

Other evidence for waves can be sought both in terms of direct measurements of fluctuations in  $\mathbf{B}$ ,  $\mathbf{b}$ , and  $n$  in the corona, but also in terms of signatures in the particle distributions and waves observed in the solar wind. These signatures are discussed briefly in later lectures on the solar wind. Suffice it is say that clear evidence does not exist and that the lack of evidence casts doubt on waves being the dominant source of heating for the corona.

#### 7.4.4 Joule heating

Magnetic loops in the solar corona are anchored in the photosphere, and the footpoints of loops are continuously displaced by photospheric flows. These displacements produce electric currents flowing in the corona, as might the spatial gradients in  $\mathbf{B}$  for loops (via  $\nabla \times \mathbf{B} = \mu_0 \mathbf{J}$ ) and confinement problems in loops, and in principle Ohmic dissipation could be responsible for coronal heating [Klimchuk, 2006]. Indeed, large scale currents  $I \approx 10^{12}$  A are inferred from vector magnetograph measurements in active regions. An observational test of the Ohmic heating hypothesis was performed by Metcalf et al. (1994), who examined the spatial and temporal relationship between soft X-ray coronal structures in an active region and the vertical current density derived from photospheric vector magnetograms. They found no convincing correlation between the vertical current sites and the observed bright X-ray structures.

The basic problem is that classical Ohmic heating is too small if the current is distributed over observed scales. The volumetric heating rate due to a field-aligned current density  $J_{\parallel}$  is  $\varepsilon_H = \sigma^{-1} J_{\parallel}^2$ , where  $\sigma$  is the conductivity. The classical (Spitzer) conductivity is

$$\sigma \approx 1.5 \times 10^{-3} T^{3/2} \text{ ohm}^{-1} \text{ m}^{-1}, \quad (7.4)$$

Accordingly if  $J_{\parallel}$  is increased, by filamenting the current into smaller area channels, then the Ohmic dissipation could be increased substantially. This would lead to larger relative electron-ion drifts and so likely a larger role for kinetic instabilities and associated wave heating.

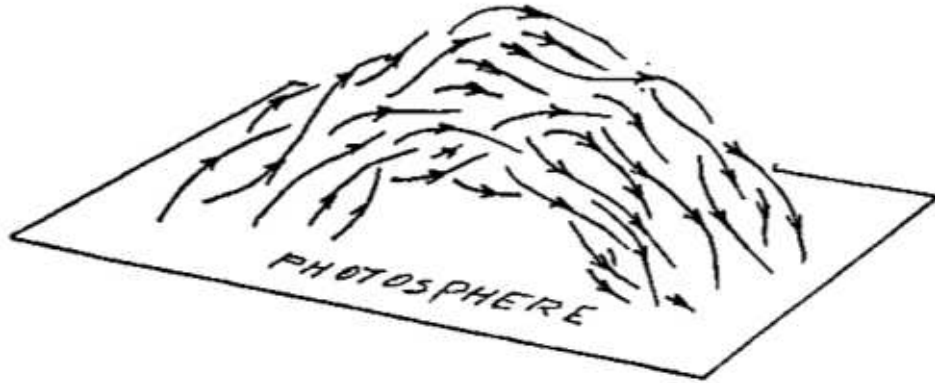


Figure 7.15: Parker’s [1988] idea of the formation of discontinuities in the corona due to the shuffling of the footpoints of field lines.

### 7.4.5 Magnetic reconnection

Last but not least we come to magnetic reconnection. At its simplest level this involves two equally-sized regions with anti-parallel magnetic field lines of equal strength  $B$  but being brought together. If the fields are superposed then  $\mathbf{B}_{tot} = 0$  and there is now zero magnetic field energy. But where has the non-zero initial magnetic energy gone? Conservation of energy demands that the initial magnetic energy is retained by the plasma, as a combination of enhanced directed kinetic energy (flow) and random thermal energy. That is, magnetic reconnection involves conversion of magnetic energy into heating and increased flow energy.

A more detailed discussion of the physics of magnetic reconnection is deferred to Lecture 9 on solar activity. Here we note that abundant evidence exists for magnetic reconnection being important on the Sun. This includes impulsive jets seen in UV and X-ray data associated with the granulation cells and the chromosphere, as well as solar flares and coronal mass ejections (Lecture 9).

One idea, due to Parker [1988] is of “nanoflares” (Figure 7.15). This involves photospheric motion of field lines causing braiding and motions of field lines in the corona, leading to regions with anti-parallel magnetic field lines (or at least an anti-parallel component of  $\mathbf{B}$ ) being brought together. This leads to magnetic reconnection and associated heating and flows. If there are enough nanoflares (or more generally, similar “flares” across a wide variety of spatial scales and so total energy releases, then there may be enough energy released to heat the corona.

Reconnection naturally leads to a strong connection between heating events and magnetic field structures in the solar atmosphere and below, qualitatively consistent with the observational constraints. Does it happen enough, however? Research continues on whether magnetic reconnection is the dominant mechanism for heating the corona, how it occurs, and whether wave heating in the reconnection regions is important.

*Acknowledgement* These lecture notes are based in part on a lecture by Dr Mike Wheatland, itself constructed on the basis of an outline of mine.

### References

Aschwanden, M.J. 2008, in *Waves & Oscillations in the Solar Atmosphere: Heating and Magneto-Seismology*, *Proceedings IAU Symposium No. 247*, eds. R. Erdélyi & C.A.

- Mendoza-Briceño, International Astronomical Union, p. 257
- Cranmer, S.R. 2009, Coronal holes, [airXiv:0909.2847v1](https://arxiv.org/abs/0909.2847v1) (15 Sept 2009)
- Cranmer, S.R., Field, G.B., and Kohl, J.L. 1999, *Astrophysical Journal* **518**, 937
- Fisher, G.H., Longcope, D.W., Metcalf, T.R. and Pevtsov, A.A. 1998, *Astrophysical Journal* **508**, 885
- Golub, L. and Pasachoff, J.M. 1997, *The Solar Corona*, Cambridge University Press, Cambridge
- Klimchuk, J.A. 2006, *Solar Physics*, **234**, 41
- Metcalf, T.R., Canfield, R.C., Hudson, H.S., Mickey, D.L., Wülser, J.-P., Martens, P.C.H. and Tsuneta, S. 1994, *Astrophysical Journal*, **428**, 860
- Parker, E. 1988, *Astrophysical Journal* **330**, 474
- Parker, E. 1999, *Astrophysics and Space Science* **264**, 1
- Scudder, J.D. 1992, *Astrophysical Journal*, **398**, 319
- Ulmschneider, P., and Kalkofen, W. 2003, in *Dynamic Sun*, ed. B.N. Dwivedi, Cambridge University Press, Cambridge, p. 181
- Withbroe, G.L. and Noyes, R.W. 1977, *Annual Reviews of Astronomy and Astrophysics*, **15**, 363